# Kinetics of Inorganic Phosphate Release during the Interaction of p21ras with the GTPase-Activating Proteins, p120-GAP and Neurofibromin†

Andrew E. Nixon,‡ Martin Brune,‡ Peter N. Lowe,§ and Martin R. Webb*,‡

*National Institute for Medical Research, The Ridgeway, Mill Hill, London, NW7 1AA, U.K., and Department of Cell Biology, Wellcome Research Laboratories, Beckenham, Kent, BR3 3BS, U.K.*

*Received June 1, 1995; Revised Manuscript Received September 21, 1995*⊗

ABSTRACT: The rate of GTP hydrolysis on p21ras is accelerated by $\sim 10^5$ times by the catalytic domains of GTPase-activating proteins (GAPs), p120-GAP (GAP-344) or neurofibromin (NF1-334). The kinetic mechanism of this activation has been investigated by following the release of inorganic phosphate ($P_i$), using a fluorescent probe that is sensitive to $P_i$ [Brune, M., Hunter, J., Corrie, J. E. T., & Webb, M. R. (1994) *Biochemistry 33*, 8262−8271]. Measurements were made in real time with a stopped-flow apparatus, in which the p21ras complex with the 2′,3′-methanthraniloyl analogue of GTP (mantGTP) was mixed with the GAP in the presence of this $P_i$ probe. The results show that $P_i$ release is fast and that the overall hydrolysis is contrlled by the cleavage itself or a conformational change preceding the cleavage. The time courses were single exponentials over a range of [GAP-344] and were modeled to show that a single step controlled $P_i$ release. The maximum rate constant was 15 $s^{-1}$ (all data at 30 °C, pH 7.6, low ionic strength) in experiments in which GAP-344 underwent a single turnover, compared with 5 $s^{-1}$ for multiple-turnover experiments, and possible causes of this discrepancy were investigated and discussed. With NF1-334 the time courses were more complex, showing a lag prior to rapid release of $P_i$. The results were consistent with a $K_d$ of 0.04 $\mu$M for NF1-334 binding to the p21ras·mantGTP complex, and two steps partially contributing to the overall rate. This NF1-344 affinity is some 3 orders of magnitude tighter than that of GAP-344. The cleavage rate at saturating NF1-334 increases from ~10 to 30 $s^{-1}$ as the ionic strength increases to physiological, although the interaction between NF1-334 and p21ras weakens with increasing ionic strength. The data are interpreted with GTP hydrolysis occurring uncoupled from any transduction, such that once the GAP interacts with p21ras, the hydrolysis (deactivation) occurs at the maximum rate possible due to the catalytic mechanism.

The Ras superfamily comprises low molecular weight (18−25 kDa) monomeric guanine nucleotide binding proteins, with homology to the proteins encoded by the Ras proto-oncogenes. There are three isoforms of the ras proteins (p21ras), Harvey, Kirsten, and N, each having a molecular weight of 21 kDa and a slow, intrinsic GTPase activity. They are modified at the C-terminus by addition of hydrophobic group(s) which locate them at the plasma membrane where they are involved in a cell-signaling pathway responsible for activation of processes important to cell growth and differentiation. There are several reviews of this system [e.g., Grand and Owen (1991), Bollag and McCormick (1991), and Wittinghofer and Pai (1991)].

Recently, signal pathways involving p21ras have been outlined, in which receptor activation leads to activation of a series of protein kinases [reviewed by Boguski and McCormick (1993), Schlessinger (1993), Marshall (1993), and Prendergast and Gibbs (1994)]. p21ras is thought to act as a molecular switch, the GTP-bound form being the biologically active conformation and the GDP-bound form inactive. This switch may be regulated by proteins that either control the rate at which the nucleotide bound to p21ras is exchanged (guanine nuceotide release factors) or stimulate the intrinsic hydrolysis reaction (GTPase-activating proteins, GAPs).[1] Two proteins of this latter group, p120-GAP and neurofibromin, have been identified from mammalian sources, and their genes have been cloned and expressed. p120-GAP was first identified by its ability to accelerate the slow intrinsic GTPase activity of p21ras and thus to down-regulate signaling through p21ras. Neurofibromin was first identified as the locus of mutations associated with neurofibromatosis type 1 and subsequently shown to have p21ras GTPase-activating activity. There is also evidence that GAPs may function as effector molecules for p21ras.

Certain single-point mutations are sufficient for production of oncogenic p21ras (Barbacid, 1987). Such activation is found in ~30% of all human tumors, and by far the most common position to be altered in the ras sequence is position 12. The effect of such mutations is thought to be the constitutive activation of signaling downstream of p21ras by maintenance of elevated levels of p21ras·GTP. This is achieved by reduction in GTPase activity especially because

† This work was supported by a European Community Twinning Grant, the Human Frontiers Science Program, and the Medical Research Council, U.K.

* To whom correspondence should be addressed. Tel.: (44) 181 959 3666. FAX: (44) 181 906 4477.

‡ National Institute for Medical Research.

§ Wellcome Research Laboratories.

⊗ Abstract published in *Advance ACS Abstracts,* November 1, 1995.

[1] Abbreviations: GAP, GTPase-activating proteins in general (p120-GAP and neurofibromin); GAP-344, the C-terminal domain of the GTPase-activating protein that has molecular weight 120 kDa; NF1-334, the C-terminal domain of neurofibromin; MESG, 2-amino-6-mercapto-7-methylpurine ribonucleoside; PBP, phosphate-binding protein; MDCC, *N*-[2-(1-maleimidyl)ethyl]-7-(diethylamino)coumarin-3-carboxamide.

0006-2960/95/0434-15592$09.00/0 

Scheme 1

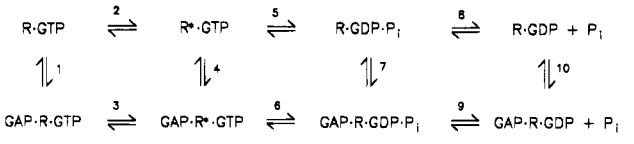


of insensitivity toward the actions of the GAPs (Trahey & McCormick, 1987; Lowe & Skinner, 1994). Some mutations *in vitro* that increase the rate of nucleotide exchange also result in oncogenic p21ras [e.g., Reinstein et al. (1991)].

In order to understand the mechanism of p21ras regulation we have investigated the mechanism of activation of p21ras·GTP hydrolysis *in vitro* by p120-GAP and neurofibromin using the C-terminal, catalytic domains of these GAPs, GAP-344 and NF1-334, respectively, expressed in *Escherichia coli* (Skinner et al., 1991; Eccleston et al., 1993). Most of the rate constants have already been determined for a minimal mechanism of the nonactivated hydrolysis of GTP by p21ras (Neal et al., 1988). The major pathway of the GAP-activated p21ras GTPase and the importance of particular states are not clear. The main molecular states of the GAP-activated p21ras GTPase are shown in Scheme 1, where R represents p21ras and GAP represents p120-GAP or neurofibromin. Steps in the mechanism are numbered, and the forward and reverse rate constants for step $i$ are $k_{+i}$ and $k_{-i}$, respectively. The conformational change to the R·GTP (step 2) was proposed on the basis of fluorescence changes to a GTP analogue, 2′(3′)-methylanthraniloyl-GTP (mantGTP) (Neal et al., 1990), and was shown to be accelerated by GAP-344 (step 3) (Moore et al., 1993). In terms of this model, the rate of the conformational change limits the hydrolysis reaction, at least at low concentrations of GAP-344. It is not clear at which stage GAP is released from p21ras, except it is known that equilibrium binding to R·GDP is weak: in principle, dissociation could occur at step 4, 7, or 10.

Because there have been no suitable probes, neither the role of the GDP·$P_i$ complexes nor their breakdown kinetics (step 8 and/or 9) is known, and it has not been possible to determine whether GDP·$P_i$ complexes are present as a significant proportion of the total p21ras or whether $P_i$ release plays a major role in the signal transduction. Eccleston et al. (1993) used the fluorescence properties of mantGTP to investigate early steps in the p21ras-GAP mechanism, following the changes in real time using a 1:1:1 complex of GAP·p21ras·mantGTP. Here we report direct measurements of the kinetics of $P_i$ release during p21ras·GTP hydrolysis activated by GAP-344 or NF1-334 and compare the results with those of Eccleston et al. (1993). Ligand release represents one of the major changes in the catalytic site, and for several nucleoside triphosphatases which have the hydrolysis coupled to a biological process (such as muscle contraction and ion transport), $P_i$ release is closely related to a major functional change. Thus in muscle, $P_i$ release is closely linked with the transition to a force-generating state during the ATPase cycle (Hibberd & Trentham, 1986).

The measurements described here use a fluorescent reporter protein to obtain the rate of $P_i$ release from p21ras. This protein is the A197C mutant of the *E. coli* phosphate-binding protein, labeled on the single cysteine with a fluorophore, *N*-[2-(1-maleimidyl)ethyl]-7-(diethylamino)coumarin-3-carboxamide (MDCC) (Brune et al., 1994). The labeled protein binds $P_i$ rapidly ($1.4 \times 10^8$ $M^{-1}$ $s^{-1}$, at pH 7.0, low ionic strength, 22 °C) and tightly ($K_d \approx 0.1$ $\mu$M), with a fluorescence enhancement of ~6-fold. Thus conditions can be chosen for which $P_i$ will rapidly bind to MDCC-PBP following release from p21ras, giving a fluorescence change with a time course that reflects the rate of $P_i$ release. The size of the fluorescence increase is directly related to the extent of GTP hydrolysis.

In most of the experiments described here, mantGTP was used rather than GTP in order to provide a precise comparison with the data of Eccleston et al. (1993). Use of this analogue provides an additional advantage because p21ras·mantGTP binds tighter to GAP-344 than does p21ras·GTP (as shown below) so that maximum levels of activation are more easily accessible. Measurements with mant-nucleotides interacting with the p21ras-GAP system indicate at most a 2-fold difference in rate constants compared with the natural nucleotides (Neal et al., 1990), implying that the modification at the ribose ring only slightly perturbs the system.

## EXPERIMENTAL PROCEDURES

*Proteins.* p21N-ras, the C-terminal domain of p120-GAP (GAP-344), and the C-terminal domain of neurofibromin (NF1-334) were isolated from *E. coli* expression systems (Hall & Self, 1986; Skinner et al., 1991; Brownbridge et al., 1993; Eccleston et al., 1993). The proteins were characterized as described. The p21ras·GTP or p21ras·mantGTP complexes were obtained as described by Brownbridge et al. (1993), and their concentrations were measured using the GAP-344-induced $P_i$ release, which is equimolar with the GTP bound (Webb & Hunter, 1992). The A197C mutant of the phosphate-binding protein was prepared from an *E. coli* expression system and labeled with MDCC as described by Brune et al. (1994). Purine nucleoside phosphorylase was the "bacterial" enzyme from Sigma.

*Materials.* MantGTP was synthesized, purified, and characterized using the method of Hiratsuka (1983) as described by Neal et al. (1990). MESG was prepared as described previously (Webb, 1992), except that it was purified on a silica column that was four times larger than that described, resulting in better separation from impurities.

*Measurements.* Absorbance spectra were obtained on a Beckman DU70 spectrophotometer. Fluorescence measurements were obtained on a Farrand Mk1 fluorimeter with a xenon lamp and were uncorrected for lamp intensity. Stopped-flow experiments were carried out in a HiTech SF61MX apparatus with a mercury lamp and HiTech IS-2 software. A monochromator was also used, with 5 mm slits on the exciting light and a 455 nm cutoff filter on the emission. Simulations of reaction schemes used the program KSIM (written by Dr. N. Millar). Data were fitted to theoretical curves using the HiTech software, Enzfitter (Biosoft), or Grafit (Leatherbarrow, 1992).

*Preparation of p21ras·[$^3$H]GDP.* p21ras (60 nmol) was incubated for 10 min at room temperature with [$^3$H]GDP (30 nmol; 385 GBq/mmol) in 400 $\mu$L of a solution containing 200 mM $(NH_4)_2SO_4$, 50 mM Tris·HCl, 50 mM NaCl, 40 mM EDTA, pH 7.5. The reaction was quenched by the addition of excess (50 mM) $MgCl_2$. This complex was then desalted using a PD-10 gel filtration column (Pharmacia) into 20 mM Tris·HCl, pH 7.5, 1 mM $MgCl_2$.

*Enzyme Synthesis of GTP.* A 30 $\mu$M solution of p21ras·[$^3$H]GDP in 20 mM Tris·HCl, pH 7.5, 1 mM $MgCl_2$, and 10 mM $P_i$ (total volume 280 $\mu$L) was incubated at 30 °C, and at timed intervals 30 $\mu$L aliquots were removed and prepared for analysis as described below. This was repeated in the presence of 54 $\mu$M GAP-344 or 5 $\mu$M neurofibromin.

*Analysis of Nucleotide Bound to p21ras.* Nucleotide was released from 0.1 to 1.0 nmol of p21ras by addition of an equal volume of 1% $HClO_4$, which results in denaturation of the protein. The pH was brought back to pH 4.0 by the addition of 0.5 volumes of 0.28 M NaOH, 0.12 M sodium acetate. Denatured protein and any other solid material were removed from the sample by centrifugation in an Eppendorf benchtop microfuge at 14 000 rpm for 2 min. Prior to analysis 3 nmol of GMP, 6 nmol of GDP, and 12 nmol of GTP were added as carrier nucleotides to the sample supernatant (typical volume 100 $\mu$L). Analysis of [$^3$H]GTP formation was by HPLC, using a Partsil-10 SAX anion exchange HPLC column (250 × 4.6 mm, Whatman). Elution was under isocratic conditions at a rate of 2 mL $min^{-1}$ using 0.5 M $(NH_4)_2HPO_4$, brought to pH 4.0 using HCl. Nucleotide elution was monitored by absorbance at 254 nm. Fractions (1 mL) were collected directly into 10 mL of ReadySafe scintillation cocktail (Beckman).

## RESULTS

Two different types of $P_i$ release measurements were made. In the first, p21ras·GTP (or p21ras·mantGTP) was in large excess over the GAP (GAP-344 or NF1-334) and the concentration of p21ras was varied to produce different levels of activation. Each GAP molecule goes through a repeated cycle, catalyzing GTP hydrolysis for many p21ras·GTP molecules. This is equivalent to a steady-state reaction, with p21ras·GTP being the substrate for the GAP catalyst, and this was assumed to follow Michaelis–Menten kinetics. These measurements were done as previously described (Webb & Hunter, 1992) using a spectroscopic assay for $P_i$ based on purine nucleoside phosphorylase and a nucleoside analogue, MESG, that has an absorbance change at 360 nm (Webb, 1992). By measuring the rate of $P_i$ release as a function of [p21ras·mantGTP], a $k_{cat}$ of 5.0 ± 0.2 (S.E.M.) $s^{-1}$ and $K_m$ of 24 ± 3 $\mu$M were obtained at pH 7.6, 30 °C, low ionic strength. This is a similar value of $k_{cat}$ to that obtained with the natural substrate, but the $K_m$ is lower than with GTP (58 ± 7 $\mu$M), suggesting that the p21ras·mantGTP binds about 2-fold tighter to GAP than does p21ras·GTP. Using this type of assay it was not possible to go to low enough concentrations to determine a $K_m$ for neurofibromin, although the $k_{cat}$ was measured as 6 $s^{-1}$, for both p21ras·mantGTP and p21ras·GTP.

In the other type of $P_i$ release measurement, GAP is in excess over p21ras·mantGTP, so that the reaction is single turnover in all components and the course of the reaction is measured in real time in a stopped-flow apparatus. When GAP-344 is rapidly mixed with p21ras·mantGTP in the presence of the fluorescent-labeled phosphate-binding protein, MDCC-PBP, the $P_i$ release following hydrolysis is measured by the fluorescence change (Figure 1). These data fit single exponentials with rate constants increasing with [GAP-344] and saturating at high [GAP-344] (Figure 2). Because the data show a single exponential, the rate of $P_i$ release is controlled by a single rate constant and so these

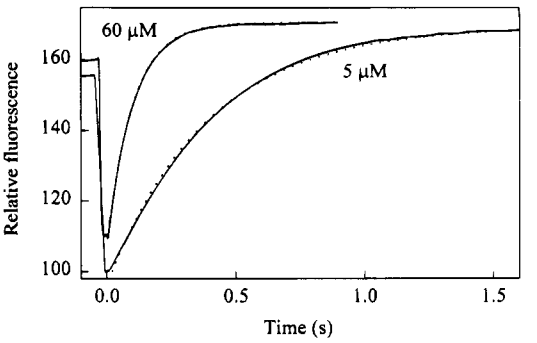


FIGURE 1: The kinetics of $P_i$ release during single-turnover hydrolysis of p21ras·mantGTP by GAP-344. Solutions in 20 mM Tris·HCl, 1 mM $MgCl_2$, pH 7.5, were mixed in the stopped-flow apparatus at 30 °C. Each solution contained 5 $\mu$M MDCC-PBP, 0.2 mM 7-methylguanosine, and 0.1 unit of purine nucleoside phosphorylase/mL. The following concentrations are those in the mixing chamber: solution 1, 1 $\mu$M p21ras·mantGTP; solution 2, GAP-344 at the concentration shown. The solid lines are experimental, the dashed lines are best-fit single exponentials.

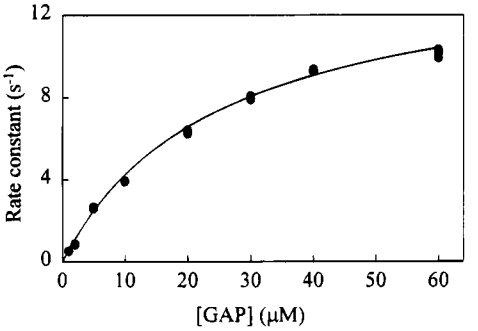


FIGURE 2: Dependence of rate of single-turnover hydrolysis on GAP-344 concentration. The best-fit single exponentials from measurements as in Figure 1 were plotted as a function of [GAP-344]. The line is the best fit to the model in eq 1, assuming that the binding is rapid. This gives a maximum rate of 15 $s^{-1}$, and $K_m$ is 25 $\mu$M.

data were fitted to the simpler model in eq 1, where it is assumed that there is rapid equilibrium binding to form the ternary complex ($K_d$ = 25 $\mu$M), followed by slow reaction ($k$ = 15 $s^{-1}$):

$$\text{GAP} + \text{R·mantGTP} \overset{K_d}{\rightleftharpoons} \text{GAP·R·mantGTP} \overset{k}{\rightarrow} \text{GAP} + \text{R·mantGDP} + P_i \quad (1)$$

In order to use the full capacity of the reporter MDCC-PBP and make quantitation easier, these measurements were done in the presence of a "$P_i$ mop" consisting of 7-methylguanosine and purine nucleoside phosphorylase (Brune et al., 1994). This removes virtually all free $P_i$ contamination from the glassware and solution by forming ribose 1-phosphate. This reaction can be made much slower than the binding of $P_i$ to MDCC-PBP so that it does not interfere with the fluorescence signal change. However, the mop does slowly remove $P_i$ from the MDCC-PBP, explaining the slow reduction of fluorescence at long times and the variable fluorescence in the premix period (negative times): the old solution in the mixing chamber has a fluorescence intensity that depends on the age of the solution since the previous mix.

This set of measurements was repeated with NF1-334 as activator. At 1 $\mu$M p21ras·mantGTP, the observed rate was independent of [NF1-334] in the range 1–10 $\mu$M, so the

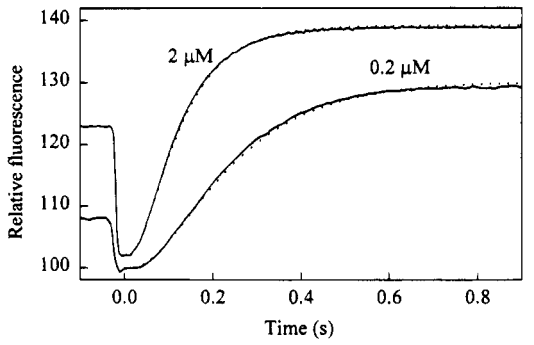


FIGURE 3: The kinetics of $P_i$ release during single-turnover hydrolysis of p21ras·mantGTP by NF1-334. The reaction was as in Figure 1, except that 0.1 $\mu$M p21ras·mantGTP and either 0.2 or 2 $\mu$M NF1-334 and 1 $\mu$M MDCC-PBP were used. The $P_i$ release predicted by the model described in the text is shown as the dashed lines.

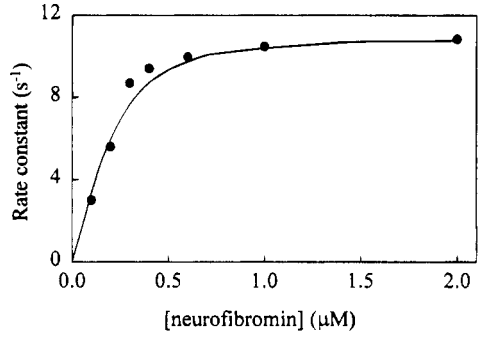


FIGURE 4: Rate of $P_i$ release as a function of NF1-334 concentration. Data were collected as in Figure 3, and the rise in fluorescence following the lag was fitted to a single exponential. The curve is for the model in Scheme 2, as described in the text. The simulations as in Figure 3 were done for the whole range of [NF1-334], and the rise in fluorescence for the second half of each time course (in terms of fluorescence intensity) was fitted to a single exponential.

measurements were also done at 0.1 $\mu$M p21ras·mantGTP in order to measure a $K_d$ value. The curves had shapes similar to those at higher [p21ras] but different from those with GAP-344 as now there is a definite lag phase after mixing, followed by an approximately exponential rise in fluorescence (Figure 3). This indicates that NF1-334 and GAP-344 are different in the activation kinetics apart from the much tighter binding of NF1-334 to p21ras: this will be analyzed in the Discussion. At 0.1 $\mu$M p21ras·mantGTP, there was a reduction in rate at low [NF1-334] (Figure 4). The rises in fluorescence were fitted to single exponentials, and the best-fit rate at high [NF1-334] gives a maximum rate of 11 $s^{-1}$.

All the above measurements were at low ionic strength, because the interaction of GAPs and p21ras decreases with ionic strength. The salt dependence of the $P_i$ release was measured by repeating the single-turnover measurements at 1 $\mu$M p21·mantGTP and 5 $\mu$M NF1-334 at different concentrations of NaCl (Figure 5). This dependence is almost identical to that observed by Eccleston et al. (1993) measuring the mant fluorescence change and shows a small rise in the rate constant as [NaCl] increases to 150 mM, after which the NF1-334 is presumably no longer saturating and the observed rate constant decreases. Another set of data was obtained at 35 $\mu$M NF1-334, so that the p21ras was saturated over a wider range of [NaCl]. These data showed a 3-fold increase in the rate constant to ~30 $s^{-1}$ as the NaCl increases to 200 mM.

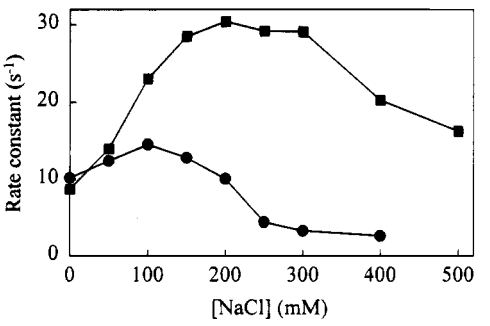


FIGURE 5: Salt dependence of the kinetics of $P_i$ release from p21ras·mantGTP at high concentrations of NF1-334. Data were collected as in Figures 1 and 4, at 1 $\mu$M p21ras·mantGTP and 5 $\mu$M (circles) or 35 $\mu$M (squares) NF1-334, with a range of added [NaCl]. The data were fitted to single exponentials: the points represent the average of at least three measurements, and the lines join the experimental points.

At maximum activation by GAP-344, there is a 3-fold difference between the rates measured in the steady state (5 $s^{-1}$) and in a single turnover (15 $s^{-1}$). However, there is no difference between the value of $K_m$ (steady state) and $K_d$ (single turnover), although the $K_m$ probably approximates to a $K_d$ because the $k_{cat}$ is likely to be much slower than the dissociation of GAP-344 from p21ras ($k_{-1}$) (see Discussion). A possible cause of the difference in maximal rates is a slow step in the GAP-activation cycle of Scheme 1, following $P_i$ release (so not affecting the single-turnover measurement) but prior to GAP binding to another p21ras·mantGTP complex (thus slowing the steady-state rate). (Note that the very slow step of unactivated nucleotide release from p21ras does not come into this cycle, as the p21ras is fully complexed with mantGTP at the start of each measurement and there is no free mantGTP). A possible slow step could be dissociation of GAP after $P_i$ release or a conformation change, for example. To test this we measured in the stopped-flow apparatus whether there was a burst of $P_i$ release in the first cycle of hydrolysis, prior to slower steady-state hydrolysis. This was done with excess p21ras·mantGTP over neurofibromin or GAP-344. Figure 6 shows the traces obtained. With NF1-334, there is a lag following mixing, and then a fairly linear hydrolysis: there is no rapid burst, and so there is no slow step following $P_i$ release. There is similarly a linear trace with GAP-344, but for this measurement a high concentration of p21ras·mantGTP (70 $\mu$M) was used to achieve high activation. This resulted in a very small amount of free $P_i$, which then gave a small burst on binding to MDCC-PBP in the mixing chamber. There is no rapid phase with an amplitude similar to [GAP-344] and rate constant ~15 $s^{-1}$. These measurements show that for either GAP, the rate of $P_i$ release in the first turnover is the same as in subsequent turnovers.

A third type of experiment was done to probe the hydrolysis and $P_i$ release reactions. This was based on the observation for many enzyme reactions that the on-enzyme equilibrium constant for the chemical step is close to unity. In particular, the myosin ATPase reaction has an equilibrium constant of [myosin·ADP·$P_i$]/[myosin·ATP] = 1−10, depending on conditions (Trentham et al., 1976; Hibberd & Trentham, 1987). This is reflected in the ability to observe ATP synthesized on the protein following addition of ADP

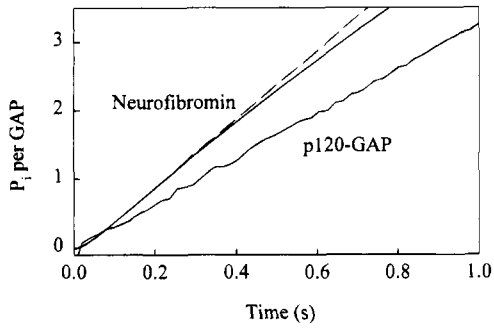


FIGURE 6: Kinetics of $P_i$ release during several turnovers of p21ras•mantGTP, with NF1-334 and GAP-344. Data were collected as described in Figure 1, but there was 10 $\mu$M p21ras•mantGTP and 1 $\mu$M NF1-334, with 10 $\mu$M MDCC-PBP. The [$P_i$] scale was calculated from the final fluorescence change, and the known percent activity of the MDCC-PBP: i.e., the total fluorescence change was 7.5 $\mu$M. The dashed line is the fit to the model described in the text, with the neurofibromin assumed to be 65% active. For the GAP-344 measurement, all of the MDCC-PBP was in the GAP syringe only, as a high protein concentration was already present in the p21ras syringe. The mixing chamber concentrations were 70 $\mu$M p21ras•mantGTP, 0.5 $\mu$M GAP-344, and 10 $\mu$M MDCC-PBP.

+ $P_i$ (Mannherz et al., 1974). An equivalent experiment was tried for p21ras, both in the presence and in the absence of 54 $\mu$M GAP or 5 $\mu$M neurofibromin, by adding 10 mM $P_i$ to the p21ras•GDP complex and incubating the mixture for up to 3 h. In no case was any bound GTP found (i.e., <1.2%, based on the error in the measurement). Thus, although at micromolar concentrations of $P_i$, the ratio [R•GDP]/[R•GTP] is large (>20; Neal et al., 1988), this result suggests that [R•GDP•$P_i$]/[R*•GTP] is also large (>50), assuming that the 10 mM $P_i$ is close to saturating in terms of binding to R•GDP.

## DISCUSSION

The data presented here have used the measurement of $P_i$ release kinetics to probe the mechanism of activation of p21ras•GTP by GAPs. In particular, a new fluorescent probe for $P_i$ has been used that is based on a phosphate-binding protein (Brune et al., 1994), and because of the large signal and the rapid, tight binding of $P_i$ to this probe, real-time data with a very good signal-to-noise ratio could be obtained at 0.1 $\mu$M p21ras•GTP. Most of the work described here used mantGTP rather than GTP in order to provide a direct comparison with the real-time data of Eccleston et al. (1993), who monitored the fluorescence of the mant group, and to investigate steps up to and including the cleavage. The same solution conditions were used for both the measurements of Eccleston et al. (1993) and those described here. An additional advantage of using mantGTP is that the $K_m$ for GAP-344 is ~2-fold lower than that with GTP, making high levels of activation more easily accessible experimentally.

The single-turnover data with GAP-344 (Figure 1) were well fitted by single exponentials. The rate constant at maximum activation (15 $s^{-1}$) is very similar to that obtained by Eccleston et al. (1993) following changes in fluorescence of mant-nucleotides and is either controlled by the hydrolysis step or by the preceding conformation change. The complete absence of a lag and the single-exponential $P_i$ release shows that there is a single elementary process controlling $P_i$ release, and it is likely that all other processes from GAP binding to $P_i$ release are much more rapid. Therefore the single step

Scheme 2

$$\text{GAP + R•GTP} \overset{1}{\rightleftharpoons} \text{GAP•R•GTP} \overset{3}{\rightleftharpoons} \text{GAP•R*•GTP} \overset{6}{\rightleftharpoons} \text{GAP + R•GDP + } P_i$$

controlling $P_i$ release is the conformation change or cleavage itself and subsequent breakdown of the GAP•p21ras•GDP•$P_i$ complex is rapid. In order to assess the extent to which a single elementary step controls the whole process, the $P_i$ release data were fitted to a model more simple than that in Scheme 1 (see Scheme 2). In this model, steps are numbered as in Scheme 1, although this requires assumptions about the major pathway of the hydrolysis mechanism: it is possible in principle that the major pathway from GAP•R*•GTP is step 4 rather than step 6. Simulations show that with $k_{+3}$ = 15 $s^{-1}$, $k_{+6}$ needs to be >100 $s^{-1}$ for there to be no predicted lag, which would be observable within the signal-to-noise ratio obtained. The data at low [GAP-344] fit $k_{+1} > 5 \times 10^6$ $M^{-1}$ $s^{-1}$ and $k_{-1} > 125$ $s^{-1}$, fulfilling the requirement of rapid binding so that there is no predicted lag. This ratio of rate constants for step 1 is required to fit the GAP-344 concentration dependence and gives a $K_d$ that is the same as the $K_m$ values obtained from the steady-state or single-turnover analyses.

The single-turnover measurements of $P_i$ release with NF1-334 are more complex, because all the traces show a lag phase immediately after mixing. When the fluorescence rise is fitted to a single exponential, saturation of the rate constant occurs at high [neurofibromin] at 11 $s^{-1}$. This is similar to the value obtained by Eccleston et al. (1993) and thus suggests that $P_i$ release is not rate limiting for the reaction up to $P_i$ release. The stopped-flow data were tested by the model in Scheme 2, and the best fits were obtained by $k_{+1} = 5 \times 10^7$ $M^{-1}$ $s^{-1}$, $k_{-1} = 2$ $s^{-1}$, $k_{+3} = 11.5$ $s^{-1}$, and $k_{+6} = 28$ $s^{-1}$ (Figure 3). The other reverse rate constants were set to 0 $s^{-1}$. In order to model the lag phase correctly, the cleavage rate and $P_i$ release must be considerably slower than with GAP-344.

The data at low [NF1-334] require the $K_d$ for NF1-334 ($k_{-1}/k_{+1}$) to be 0.04 $\mu$M in order to obtain the observed dependence on concentration. This is a more satisfactory way of estimating the affinity, rather than directly using the single-exponential fit in Figure 4. This is because the $P_i$ release curves do not fit exponentials well and the conditions at low [NF1-334] are not pseudo first order; there is no large excess of NF1-334 over p21ras•mantGTP, and so the theoretical curve based on eq 1 is not appropriate. Note that because of the slow $k_{-1}$ in the set of rate contants above, $K_m$ is calculated as $(2 + 11.5)/(5 \times 10^7)$, which is 0.27 $\mu$M and thus is an order of magnitude greater than $K_d$.

The data with GAP-344 shows a marked discrepancy between the steady-state data and the single-turnover data. The values of $K_m$ agree well, but the values of $k_{cat}$ differ markedly: 5 $s^{-1}$ from the steady-state data and 15 $s^{-1}$ from single-turnover measurements. The accuracy of these values is affected by the fact that even at the highest [GAP-344] the conditions are not saturating and by the inaccuracy of measuring active protein concentrations. The value of [p21ras] is fairly accurate as it is based on an enzyme assay of the GTP-bound form (Webb & Hunter, 1992), but [GAP] is based on total measured protein concentrations and it is not known what proportion of GAP-344 or NF1-334 is active. However, as outlined in the Results, it is possible that the difference in observed rates is due to a slow step in

the mechanism after $P_i$ release, limiting the multiple turnover of GAP in the steady-state measurement but not limiting the single turnover. Such a slow step could be release of the GAP from the GAP•p21ras•GDP complex or a conformation change. With NF1-334 there was also a difference in measured rate constants (6 $s^{-1}$ from steady-state measurements, 11 $s^{-1}$ from single-turnover measurements).

It was possible to test directly whether there was a slow step in the mechanism after $P_i$ release. This was done by following several turnovers of NF1-334 in the stopped-flow apparatus. If there is such a slow step, the first turnover of NF1-334 will be more rapid than subsequent ones, and so there would be an initial burst of $P_i$ release followed by slower steady-state reaction. Such a measurement circumvents problems with comparing steady-state data with single-turnover measurements outlined above. A rapid initial phase ("burst") was not observed (Figure 6), and so there is no slow step following $P_i$ release. In Figure 6, the best fit to the set of rate constants listed above for Scheme 2 suggests that the neurofibromin is 65% active. The steady-state $k_{cat}$ value quoted above was calculated from the (reaction velocity)/[NF1-334], assuming the neurofibromin was 100% active: using the value of 65%, the $k_{cat}$ from steady-state measurements becomes 9 $s^{-1}$, much closer to the 11 $s^{-1}$ from the single-turnover measurements.

The type of multiple-turnover measurement done with NF1-334 is not so straightforward with GAP-344 because of the high concentration of p21ras•mantGTP required to be close to saturating. However, the data from this type of experiment (Figure 6) show no sign of a burst that might be due to a rapid first turnover. There is a linear production of $P_i$ with a rate constant of 3 $s^{-1}$, close to that obtained by steady-state measurements at a similar level of activation. With GAP-344, we cannot eliminate the proportion of active protein being the source of the 3-fold difference in $k_{cat}$ values. The 3-fold difference in observed maximum rates would require that the GAP-344 was only 33% active. As suggested in the Results, if $k_{-1}$ is fast for GAP-344 then $K_d \approx K_m$. The $K_d$ = 25 $\mu$M quoted from the single-turnover measurements assumes that the GAP-344 is 100% active. The measurement of $K_m$ = 24 $\mu$M from the steady-state measurements is independent of GAP activity but depends on the p21ras•GTP concentration, which was calculated based on total $P_i$ formation on hydrolysis of bound GTP or mantGTP and thus is likely to be accurate. These constants therefore imply that the GAP-344 is close to 100% activity. One way out is if $k_{-1}$ is slow (and so $K_m \neq K_d$), but modeling predicts a significant lag (not observed) if the rate constants are adjusted to allow such a slow dissociation.

Thus it currently does not seem that consideration of the proportion of active protein will explain the discrepancy in maximum rates for GAP-344. Other possible explanations for the difference between single- and multiple-turnover rates are an unknown complexity in the mechansim and the fact that multiple-turnover measurement at high activation requires high concentrations of p21ras whereas the single-turnover measurements are at low concentration of p21ras. This protein may aggregate at high concentrations (Hazlett et al., 1993, and references therein) and so possibly alter its kinetic mechanism, giving rise to the observed differences; however, there is no direct evidence for such an explanation.

The high sensitivity of the fluorescent $P_i$ probe has enabled accurate assessments to be made of the dissociation constants of both neurofibromin ($K_d$ = 0.04 $\mu$M) and GAP-344 (25 $\mu$M) with p21ras•mantGTP using real-time kinetic measurements. Thus there is a difference of almost 3 orders of magnitude between the affinity of the two GAPs for p21ras. Apart from the large difference in affinities, there are also differences in other parts of the kinetic mechanism that manifest themselves in the lag. This requires the cleavage and $P_i$ release steps to be slower with NF1-334 than with GAP-344. There is only a small difference in the kinetics of the rate-limiting process, and hence in the maximal rates.

The salt dependence of $P_i$ release in the neurofibromin-activated reaction shows a 3-fold increase in the observed rate on increasing to 200 mM NaCl, presumably due to an increase in $k_{+3}$ of Scheme 2, which is the rate-limiting rate constant at saturating neurofibromin. Thus the process controlling the cleavage is optimized at physiological ionic strength, although the neurofibromin may not saturate at physiological concentrations (it should be borne in mind, however, that p21ras is bound to the membrane in the cell, and so the concentration effects found in solution are not directly comparable). The decrease in observed rate at higher [NaCl] is consistent with the salt weakening the interaction of proteins: the conditions used are no longer saturating, and the observed rate constant is determined by the extent of interaction between proteins. This may have implications for the role of neurofibromin. If the neurofibromin is saturating, then a change in concentration of active neurofibromin by some control mechanism will not change the rate of deactivation of p21ras•GTP. If the neurofibromin is not saturating then the control of active concentration of neurofibromin can regulate the rate of p21ras GTP hydrolysis between 30 and 0 $s^{-1}$.

The data presented here show that $P_i$ release is rapid during the GAP-activated hydrolysis. There is very little bound $P_i$ at any time. The data show that, although the $k_{cat}$ values for the two GAPs are similar, there are distinct differences between the kinetic mechanisms of GAP-344 and NF1-334, apart from the difference in affinities. For neither of the GAPs has it yet been possible to correlate $P_i$ release with dissociation of the GAP from p21ras in terms of order of dissociation or relative rates. It seems likely that they are both rapid processes: there is no evidence for a slow process following $P_i$ release. The cellular roles of the GAPs remain elusive. If they are solely negative regulators, they will activate the GTP hydrolysis in way that is uncoupled from the signal transduction. This may be equivalent the situation with actomyosin. In muscle fibers the hydrolysis is coupled to energy transduction, but with isolated actomyosin subfragment 1 in solution the hydrolysis is uncoupled. In the latter case, $P_i$ release is rapid (Brune et al., 1994); in fibers, $P_i$ release kinetics are slower and this biochemical process is closely linked with the transition from a low-force state to a high-force state (Hibberd & Trentham, 1986). Indeed the rate for actomyosin in solution is similar to that for GAP-activated hydrolysis. Thus it appears that GAPs may operate by binding to p21ras and deactivating at a maximum rate allowed by the enzymic mechanism.

## ACKNOWLEDGMENT

We thank Dr. R. Skinner (Wellcome Research Laboratories) for the expression systems for NF1-334 and GAP-344.

## REFERENCES


Barbacid, M. (1987) *Annu. Rev. Biochem. 56*, 779−827.

Boguski, M. S., & McCormick, F. (1993) *Nature 366*, 643−654.

Bollag, G., & McCormick, F. (1991) *Annu. Rev. Cell Biol. 7*, 601−632.

Brownbridge, G. G., Lowe, P. N., Moore, K. J. M., Skinner, R. H., & Webb, M. R. (1993) *J. Biol. Chem. 268*, 10914−10919.

Brune, M.; Hunter, J., Corrie, J. E. T., & Webb, M. R. (1994) *Biochemistry 33*, 8262−8271.

Eccleston, J. F., Moore, K. J. M., Morgan, L., Skinner, R. H., & Lowe, P. N. (1993) *J. Biol. Chem. 268*, 27012−27019.

Grand, R. J. A., & Owen, D. (1991) *Biochem. J. 279*, 609−631.

Hall, A., & Self, A. J. (1986) *J. Biol. Chem. 261*, 10963−10965.

Hazlett, T. L., Moore, K. J. M., Lowe, P. N., Jameson, D. M., & Eccleston, J. F. (1993) *Biochemistry 32*, 13575−13583.

Hibberd, M. G., & Trentham, D. R. (1986) *Annu. Rev. Biophys. Biophys. Chem. 15*, 119−161.

Hiratsuka, T. (1983) *Biochim. Biophys. Acta. 742*, 496−508.

Leatherbarrow, R. J. (1992) *Grafit Version 3.0*, Erithacus Software Ltd., Staines, U.K.

Lowe, P. N., & Skinner, R. H. (1994) *Cell. Signalling 6*, 109−123.

Mannherz, H. G., Schenk, H., & Goody, R. S. (1974) *Eur. J. Biochem. 48*, 287−295.

Marshall, M. S. (1993) *Trends Biochem. Sci. 18*, 250−254.

Moore, K. J. M., Webb, M. R., & Eccleston, J. F. (1993) *Biochemistry 32*, 7451−7459.

Neal, S. E., Eccleston, J. F., Hall, A., & Webb, M. R. (1988) *J. Biol. Chem. 263*, 19718−19722.

Neal, S. E., Eccleston, J. F., & Webb, M. R. (1990) *Proc. Natl. Acad. Sci. U.S.A. 87*, 3562−3565.

Prendergast, G. C., & Gibbs, J. B. (1994) *BioEssays 16*, 187−191.

Reinstein, J., Schlichting, I., Frech, M., Goody, R. S., & Wittinghofer, A. (1991) *J. Biol. Chem. 266*, 17700−17706.

Schlessinger, J. (1993) *Trends Biochem. Sci. 18*, 273−275.

Skinner, R. H., Bradley, S., Brown, A. L., Johnson, N. J. E., Rhodes, S., Stammers, D. K., & Lowe, P. N. (1991) *J. Biol. Chem. 266*, 14163−14166.

Trahey, M., & McCormick, F. (1987) *Science 238*, 542−545.

Trentham, D. R., Eccleston, J. F., & Bagshaw, C. R. (1976) *Q. Rev. Biophys. 9*, 217−281.

Webb, M. R. (1992) *Proc. Natl. Acad. Sci. U.S.A. 89*, 4884−4887.

Webb, M. R., & Hunter, J. L. (1992) *Biochem. J. 287*, 555−559.

Wittinghofer, A., & Pai, E. F. (1991) *Trends Biochem. Sci. 16*, 382−387.


BI9512298